

Advances in Spherical Harmonic Device Modeling: Calibration and Nanoscale Electron Dynamics

Chung-Kai Lin, Neil Goldsman, Isaak Mayergoyz, Sheldon Aronowitz* and Nadya Belova*
Dept. of Electrical Engineering, University of Maryland, College Park, MD 20742, USA

*LSI Logic Corp. Milpitas CA

Email: cklin@glue.umd.edu, neil@glue.umd.edu Fax:+1-301-3149281 Phone:+1-301-4053648

Abstract: Improvements in the Spherical Harmonic (SH) method for solving Boltzmann Transport Equation (BTE) are presented. The simulation results provide the same physical detail as analytical band Monte Carlo (MC) calculations, and are obtained approximately a thousand times faster. A new physical model for surface scattering has also been developed. As a result, the SHBTE model achieves calibration for a complete process of I-V characteristics and substrate current consistently for the first time.

1. Introduction

The Spherical Harmonic Boltzmann Transport Equation (SHBTE) method achieves device simulation by direct self-consistent solution to the Boltzmann transport equation (BTE) and the Poisson equation[1,2]. It gives the distribution function for the device approximately one thousand times faster than the analytical band Monte Carlo (MC) method and without statistical noise. It does not suffer from the same assumptions as the drift-diffusion (DD) and hydrodynamic (HD) models. In response to these attributes, industry is beginning to employ the method. However, questions remain concerning truncation error, agreement with Monte Carlo simulation, the ability of the SHBTE to capture the electron dynamics under highly rapid variations of electric field, and its applicability to process and device calibration.

In this work, we demonstrate that the SHBTE model agrees with MC for the distribution function. We also improve the model to account for truncation error and to ensure capture of electron dynamics for fields varying on dimensions as small as $0.01\mu\text{m}$. We also improved the surface scattering model to help facilitate process calibration of both I-V characteristics and substrate current with one self-consistent SHBTE model. We obtain agreement with experiment for substrate current without using any fitting parameters! (This is in contrast with DD and HD models, which do not calculate the distribution function thereby forcing substrate current to be calculated using ad-hoc models.)

2. Expansion Truncation and Nanoscale Electron Dynamics:

We start our discussion with Boltzmann Transport Equation:

$$\frac{1}{\hbar} \nabla_{\vec{k}} \varepsilon \cdot \nabla_{\vec{r}} f(\vec{r}, \vec{k}) + \frac{q}{\hbar} \nabla_{\vec{r}} \phi(\vec{r}) \cdot \nabla_{\vec{k}} f(\vec{r}, \vec{k}) = \left. \frac{\partial f(\vec{r}, \vec{k})}{\partial t} \right|_{coll} \quad (1)$$

where $\phi(\vec{r})$ is the potential; $f(\vec{r}, \vec{k})$ is the electron distribution function; ε is the energy; \vec{k} is the electron wave-vector; \vec{r} is the position vector; \hbar is Planck's constant. With the SH method the distribution function is expressed as a spherical harmonic expansion $f(\vec{r}, \vec{k}) = \sum_{l=0}^{\infty} \sum_{m=-l}^l f_l^m(\vec{r}, \varepsilon) Y_l^m(\theta, \phi)$. The expansion is then substituted into the Boltzmann equation. With Fermi's golden rule and deformation potential theory, the collision term can be expressed analytically. Mathematical manipulation transforms the BTE into a system of equations for the coefficients coupled to nearest neighbors[1]. The equations for the first two coefficients in 1-D are given below.

The zero equation:

$$-\frac{\partial}{\partial x} \left[m^* \gamma(H + q\phi) \tau(H + q\phi) v(H + q\phi) \frac{\partial F_0(x, H)}{\partial x} \right] = \left[\frac{\partial F_0(x, H)}{\partial x} \right]_{coll} \quad (2)$$

The first order equation:

$$v(x, H) \left[\frac{\partial}{\partial x} \right] F_0(x, H) + O(F_2(x, H)) = -\frac{F_1}{\tau_1} \quad (3)$$

where $H = \varepsilon - q\phi(\vec{r})$; $\frac{1}{\tau} = \frac{1}{\tau_{ac}} + \frac{1}{\tau_{op}} + \frac{1}{\tau_{imp}}$; $O(F_2)$ represents the truncation effect contributed from higher order terms. In this paper we benchmark SHBTE against MC for three different devices: one $0.075\mu\text{m}$ base

BJT; and two N^+NN^+ structures with N region lengths of $0.06\mu\text{m}$ and $0.15\mu\text{m}$ respectively. In Fig. 1 we compare the SHBTE and MC simulations for the two N^+NN^+ structures. In Fig. 1a we show the electric fields vary by more than 300kV/cm over $0.02\mu\text{m}$. In Fig. 1b we show the resulting distribution function agrees with MC calculations, and in Fig 1c we show that the velocity calculated by the SHBTE method agrees with MC calculations. (No fitting parameters are used, the MC and SHBTE have identical inputs.) In Fig 2a, we show the doping profile of the BJT, and resulting electric field with an applied potential of $V_{BE} = 0.85\text{V}$ and $V_{CB} = 3\text{V}$. (Here the electric field also varies by as much as 300kV/cm just over a distance of $0.02\mu\text{m}$.) Using the the same physical inputs, Fig. 2b shows agreement between the SH and MC results for the energy distribution functions. Agreement between the SHBTE and MC results in Figs. 1b and 2b indicates that the energy distribution function, which is the zero order term in the SH expansion, is not visibly affected by truncation for active dimensions as little as $0.06\mu\text{m}$. The only discrepancy we see is in Fig. 2c, which is a small disagreement in the velocity overshoot region of the BJT. We attribute this small disagreement to a minor truncation error in the first order term of the SH expansion. We helped to verify this by adding the second order term to our solution, and found this modification yielded better agreement. We found that the inclusion of a higher order term in the SH expansion has the effect of reducing the coefficients of the odd numbered spherical harmonics for low values of energy when the electric field is varying very rapidly in space. We find that compensation for the truncation error can be implemented by mimicking the inclusion of higher order SH terms by modifying the scattering rate in Eq(3) to be larger for lower energies when the field is rapidly varying. The modified τ can be defined as $\tau(\varepsilon_{eff}) = \tau(\varepsilon + \varepsilon_{offset})$, where ε_{offset} is given by

$$\varepsilon_{offset}(x) = \left[(\varepsilon_0 - \varepsilon(x)) \frac{E'_{max}}{E(x)} \right] \times A + \left[(\varepsilon_0 - \varepsilon(x)) \frac{E'_{max}}{4E(x)^2} \right] \times B \quad (4)$$

where $\varepsilon_0 = CE'_{max}$. $A = 0.8, B = 0.2, C = 2.66e^{-12}$
 E'_{max} =maximum electric field in device. E'_{max} =maximum of first derivative of electric field in the device. The A, B, C values are calibrated by MC for a variety structures and biases. With this compensation, we find that the SH method captures deep submicron electron dynamics without sacrificing computational efficiency. Figs. 1c and 2c show virtually perfect agreement between the corrected SH (solid-line) and MC for the deep submicron BJT and N^+NN^+ structures.

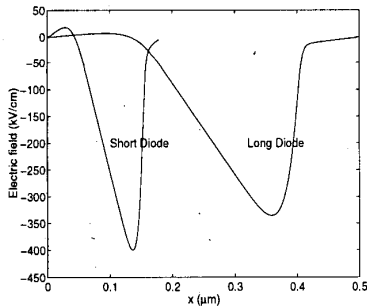


Fig. 1a

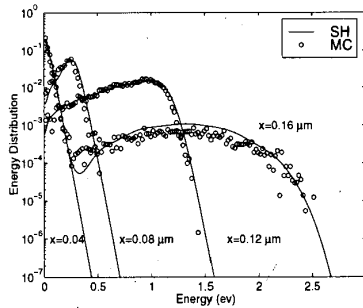


Fig. 1b

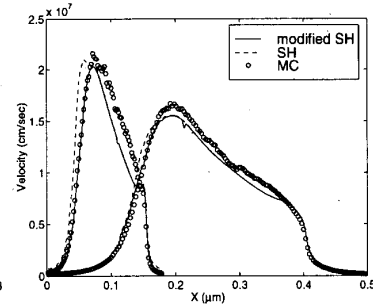


Fig. 1c

Fig. 1a: Electric fields for two different N^+NN^+ structures. The short diode has N region length of $0.06\mu\text{m}$, and the other $0.15\mu\text{m}$. Fig. 1b: Distribution function for short diode at various locations showing agreement with Monte Carlo simulation. Fig. 1c: Average velocity for both the long and short diodes, with and without scattering modification. Agreement with MC is obtained for all cases.

3. MOSFET Process Calibration:

With MC corroboration established, we now apply the model to real 2-D MOSFET simulation where we use the SHBTE to calibrate a 0.25 micron process for the first time. 2-D self-consistent simulation requires we add the Poisson and Hole Current Continuity equations to complete the SHBTE model.

$$\nabla_{\vec{r}}^2 \phi(\vec{r}) = \frac{q}{\epsilon_s} \left[\int f(\vec{k}, \vec{r}) d\vec{k} - p(\vec{r}) + N_A(\vec{r}) - N_D(\vec{r}) \right] \quad (5)$$

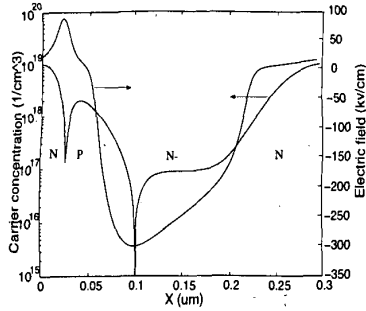


Fig. 2a

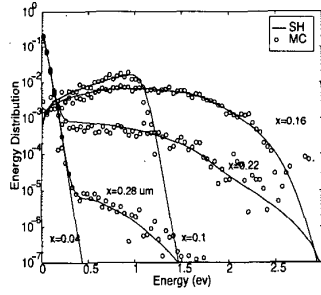


Fig. 2b

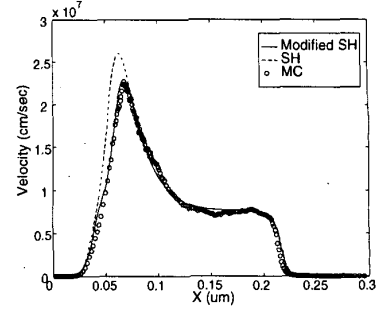


Fig. 2c

Fig. 2a: Doping profile and electric field in $0.075\mu\text{m}$ base BJT. Fig. 2b: Agreement between SH and MC for distribution function at regular locations in BJT. Fig. 2c: Average velocity with and without correction for truncation error in BJT.

$$\nabla_{\vec{r}} \cdot [\mu_p p(\vec{r}) \nabla_{\vec{r}} \phi(\vec{r}) + \mu_p V_t \nabla_{\vec{r}} p(\vec{r})] = R(\phi, n, p) - G_{ii}(\phi, n, p) \quad (6)$$

where $p(\vec{r})$ is the hole concentration; $N_A(\vec{r})$ and $N_D(\vec{r})$ is the doping concentration for acceptors and donors; ϵ_s is the silicon dielectric constant; μ_p is the hole mobility; $R(n, p)$ is the net SHR hole recombination rate; $G_{ii}(n, p)$ is the hole generation rate due to impact ionization.

We find that the SHBTE model is already fairly well suited for process calibration. However, it can be improved by revising our surface scattering rate. In previous work, the surface scattering rate was derived while accounting for surface acoustic and surface roughness scattering, with the assumption that only one quantum subband in the MOSFET inversion layer was occupied. This assumed a 2-D density of states which gave rise to the energy independent form for surface scattering $\overline{S_{inv}}(E_{\perp})$, that is explicitly dependent on the electric field perpendicular to the interface [1].

However, as device dimensions continue to shrink, higher order subbands become occupied as well, so the density of states takes on some 3-D characteristics. This will give rise to the scattering rate having an energy dependence. To account for the correction incorporating 3-D density of states, we introduce the following relationship:

$$S_{inv}(E_{\perp}, \epsilon) = \beta(E_{\perp})g(\epsilon) \quad (7)$$

where $S_{inv}(E_{\perp}, \epsilon)$ is the scattering rate corrected for higher subbands, $\beta(E_{\perp})$ is an energy independent mapping function that depends on the perpendicular electric field, and $g(\epsilon)$ is the 3-D density of states. Thus, as long as we know $\beta(E_{\perp})$, the energy and electric field dependent surface scattering rate $S_{inv}(E_{\perp}, \epsilon)$ can be obtained immediately. To obtain $\beta(E_{\perp})$, we map the 2-D scattering rate $\overline{S_{inv}}(E_{\perp})$ to the energy dependent one $S_{inv}(E_{\perp}, \epsilon)$. This is achieved by assuming that $\overline{S_{inv}}(E_{\perp})$ is the average of $S_{inv}(E_{\perp}, \epsilon)$.

$$\overline{S_{inv}}(E_{\perp}) = \frac{\int [\beta(E_{\perp})g(\epsilon)] F_0^0(\epsilon)g(\epsilon)d\epsilon}{\int F_0^0(\epsilon)g(\epsilon)d\epsilon} \quad (8)$$

where F_0^0 is the solution from Eq.(2);

$\beta(E_{\perp})$ can be obtained by rearranging (8), and factoring it out of the integral:

$$\beta(E_{\perp}) = \overline{S_{inv}}(E_{\perp}) \cdot \frac{\int F_0^0 g(\epsilon) d\epsilon}{\int F_0^0(\epsilon) g^2(\epsilon) d\epsilon} \quad (9)$$

We solve the above equation numerically for $\beta(E_{\perp})$ at each mesh point in the inversion layer. We then evaluate the product $\beta(E_{\perp})g(\epsilon)$ to obtain $S_{inv}(E_{\perp}, \epsilon)$, the scattering rate in the inversion layer that depends both on energy as well as perpendicular electric field.

Finally, in order to more accurately calibrate the entire process, especially for the shortest device, we lump contact and external measurement resistance into the effective resistance R_{ext} on the drain side. Using an iterative method, we determined R_{ext} for the process, and thereby the actual boundary condition on the drain can be obtained: $V_{d_{eff}} = V_{d_{app}} - I_d \times R_{ext}$. Using standard values for bulk phonon scattering, and taking the surface scattering rate as adjustable, we calibrate a NMOS process with three different effective gate lengths $0.88 \mu\text{m}$, $0.35 \mu\text{m}$ and $0.15 \mu\text{m}$. Fig. 3 shows all calibrated IV characteristics of these three different NMOS devices with measurement data. All the error of simulation data is within 5%.

Since the SH method gives the distribution function, it is ideal for calculating substrate current. We calculate the impact ionization rate with the random k model[3]. We then include impact ionization in the BTE's collision integral as described in [1]. Taking the electron and hole generation rates to be equal, gives rise to substrate current composed of holes. Our resulting substrate current simulation values, which are shown in Figs. 4a, 4b, and 4c, agree with experiment for all three devices without the need for any fitting parameters!

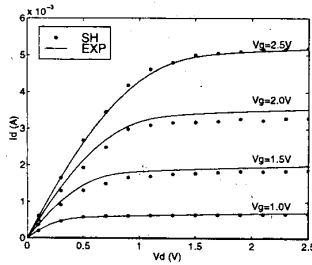


Fig. 3a

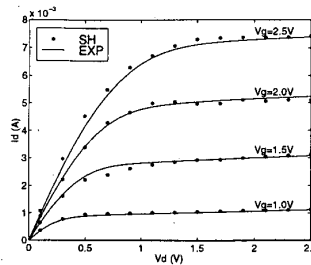


Fig 3b

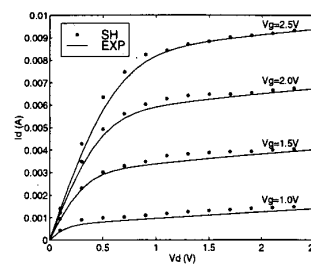


Fig. 3c.

Fig. 3: Agreement with experiment for I-V characteristics of $0.88 \mu\text{m}$ (3a), $0.35 \mu\text{m}$ (3b) and $0.15 \mu\text{m}$ (3c), effective channel length devices from a single process.

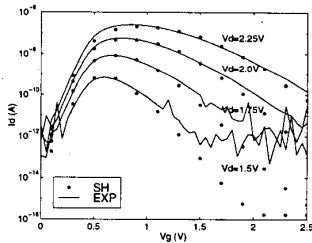


Fig. 4a

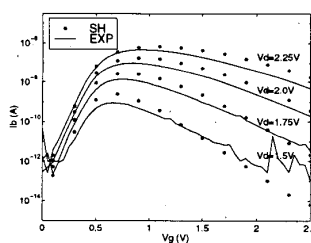


Fig. 4b

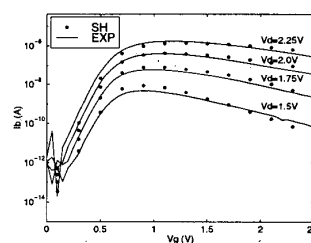


Fig. 4c

Fig. 4: Agreement with experiment for substrate current characteristics of $0.88 \mu\text{m}$ (4a), $0.35 \mu\text{m}$ (4b) and $0.15 \mu\text{m}$ (4c), effective channel length devices from a single process. No fitting parameters were used!

1. W. Liang, N. Goldsman, I. Mayergoyz, P. Oldiges, *IEEE Trans. on Elec. Dev.*, vol. 44, pp. 257-276, 1997.
2. M.C. Vecchi, J. Mohring, M. Rudan, *IEEE Trans. on CAD ICAS*, vol. 16, pp. 353, 1997.
3. Y.-J. Wu, N. Goldsman, *Journal of Applied Physics*, vol. 78, no. 8, 1995.